IEEE Access
Multidisciplinary | Rapid Review | Open Access Journal

Received September 11, 2018, accepted October 15, 2018, date of publication October 18, 2018,
date of current version November 14, 2018.

Digital Object Identifier 10.1109/ACCESS.2018.2876802

Design of A Novel Passive Binary-Controlled Variable Stiffness Joint (BpVSJ) Towards Passive Haptic Interface Application

MOHAMMAD I. AWAD[1], (Member, IEEE), DONGMING GAN[1], IRFAN HUSSAIN[1], (Member, IEEE), ALI AZ-ZU'BI[2], CESARE STEFANINI[3], (Member, IEEE), KINDA KHALAF[3], (Senior Member, IEEE), YAHYA ZWEIRI[4], JORGE DIAS[1,5], (Senior Member, IEEE), AND LAKMAL D. SENEVIRATNE[1]

[1]Khalifa University Center for Autonomous Robotic Systems, Khalifa University of Science and Technology, Abu Dhabi, United Arab Emirates
[2]Department of Mechanical Engineering, Khalifa University of Science and Technology, Abu Dhabi, United Arab Emirates
[3]Department of Biomedical Engineering, Khalifa University of Science and Technology, Abu Dhabi, United Arab Emirates
[4]Faculty of Science, Engineering and Computing, Kingston University London, London SW15 3DW, U.K.
[5]Systems and Robotics and the Faculty of Science and Technology, University of Coimbra, 3000-370 Coimbra, Portugal

Corresponding author s: Mohammad I. Awad (mohammad.awad@ku.ac.ae) and Dongming Gan (dongming.gan@ku.ac.ae)

This work was supported by the Khalifa University of Science and Technology under Khalifa University Research Internal Fund-2.

ABSTRACT In this paper we present the design, development and experimental validation of a novel Binary-Controlled Variable Stiffness Joint (BpVSJ) towards haptic teleoperation and human interaction manipulators applications. The proposed actuator is a proof of concept of a passive revolute joint, where the working principle is based on the recruitment of series-parallel elastic elements. The novelty of the system lies in its design topology, including the capability to involve an (n) number of series-parallel elastic elements to achieve (2^n) levels of stiffness, as compared to current approaches. Accordingly, the level of stiffness can be altered at any position without the need to revert to the initial equilibrium position. The BpVSJ has low energy consumption and short switching time, and is able to rotate freely at zero stiffness without limitations. Further smart features include scalability and relative compactness. This paper details the mathematical stiffness modeling of the proposed actuator mechanism, as well as the experimentally measured performance characteristics. The experimental results matched well with the physical-based modeling in terms of stiffness variation levels. Moreover, Psychophysical experiments were also conducted using (20) healthy subjects in order to evaluate the capability of the BpVSJ to display three different levels of stiffness that are cognitively realized by the users. The participants performed two tasks: a relative cognitive task and an absolute cognitive task. The results show that the BpVSJ is capable of rendering stiffness with high average relative accuracy (Relative Cognitive Task relative accuracy is 97.3%, and Absolute Cognitive Task relative accuracy is 83%).

INDEX TERMS Variable Stiffness Mechanism, Passive Haptic Interface, Psychophysical Tasks

I. INTRODUCTION

Recent research in haptic interfaces has facilitated the advancement of conveying information from remote and virtual environments. The operator's perception of the conveyed information can be obtained cutaneously (through touch) [1]–[4], or kinesthetically (through force or torque) [1]. Haptic Interfaces have a wide spectrum of applications, including navigation [5]–[8], tele-rehabilitation [9], [10], tele-surgery [11], [12], as well as micro-manipulation [13], [14]. Generally, in bilateral teleoperation, an operator can interact with a remote/virtual slave device (robot) through a haptic interface. The haptic interface typically sends the position and velocity commands to the slave device and feeds the registered contact forces back to the operator. Nonetheless, the haptic stimuli, provided by most of the commercially available haptic devices, are still limited to vibrations, reducing the possibility of simulating rich functional contact interactions [15], [16]. Towards more realistic feeling of touching virtual and remote environments, researchers have traditionally focused on grounded haptic interfaces, such as Sigma 7 [17] devices, and glove type haptic displays, such as the CyberGrasp [18].

A haptic interface typically consists of a stimuli, an actuation system, and a control system. From an actuation point of view, haptic interfaces are classified into active, passive and hybrid. An active haptic interface is equipped with actuators (motors) which are capable of adding or dissipating energy from the system. In literature, an extensive number of active haptic interfaces are presented, including the grounded type, such as the PHANTOM [19], and arm exoskeletons [20], as well as wearables, such as haptic gloves [21], [22]. Passive haptic devices, on the other hand, are incorporated with energetically passive actuators, and can hence only dissipate, store or redirect kinetic energy within a system [23]. Energy dissipative haptic devices are intrinsically safe and stable as compared to the active counterparts, but unable to restore energy [24]. By contrast, hybrid haptic devices combine both active and passive actuation, thereby achieving the safety and stability of passive actuators, and the ability to perform energy restitution of active actuators [25]. Both passive and hybrid haptic interfaces incorporate several types of energy dissipative actuators, including electromagnetic dry friction clutches [26], electro-rheological (ER) clutches [27], programmable differential breaks [28], Eddy Current Breaks [29], and MR Brakes [30].

Although energy dissipative (passive) haptic interfaces have the capability of simulating different tasks that include kinesthetic interaction with passive bodies (eg. wall following) [31], they're not able to fully simulate the interaction with passive elastic bodies. Elastic bodies (Fig. 1a) store energy during compression/elongation, but the direction of the force during the deformation process is always against the direction of motion (Fig. 1b). In this part of the interaction, an energy dissipative haptic device is capable to simulate as it can only generate forces against the motion's direction. On the other hand, this type of haptic devices cannot simulate the process of releasing as the motion and force share the same direction (fig 1c). To resolve this issue without losing the advantage of passiveness, elastic elements can be integrated within the actuation system of passive haptic interfaces. In this paper, we propose an actuator based on such a design topology. The novel Binary-Controlled Variable Stiffness Joint (BpVSJ) proposed here is to becombined with an upper limb wearable haptic stimuli, towards achieving kinesthetic interactions with the elastic element in a virtual reality environment as shown in Fig. 1d.

Realizations of incorporating elastic elements in passive haptic interfaces have been previously reported in literature. In the Elastic Arm [32], elastic cords were applied for obtaining egocentric haptic feedback through body-mounted elastic armature. Fabric stiffness has also been used in cutaneous haptic devices, such as the Bi-elastic fabric softness display [33]. A grounded passive device for real time stiffness display was introduced in [34], while serial elastic actuators (SEA) were used to enhance the closed loop behavior and reduce the output impedance [35]. The main limitations of the SEA lie in its non-optimal performance and non-optimal energy efficiency. Optimal performance requires

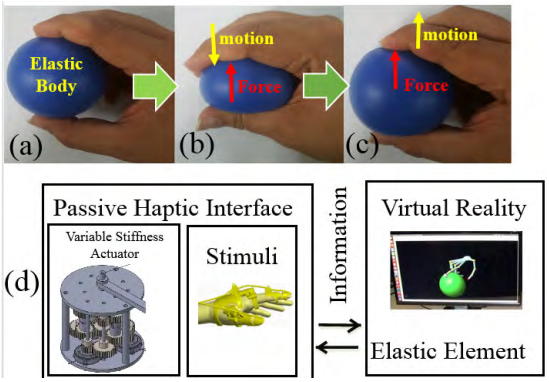

FIGURE 1. (a) Representation of kinesthetic interaction with elastic Elements, (b) During compression (c) During releasing (d) The conceptual diagram of the integration of our proposed passive binary controlled variable stiffness joint with the haptic glove to render the kinesthetic interaction with elastic element in virtual reality environment.

careful tuning of the joint stiffness values [36]. This has indeed motivated researchers to develop new designs for variable stiffness actuators.

Several topologies and realizations for Variable Stiffness Actuators have been explored in literature. Several research groups investigated the evolutionary concept of antagonistic variable stiffness actuators, where the joint stiffness is varied through the combination of two antagonistic SEAs controlled by two separate motors. Designs that fall into this category include VSA-I [37], VSA-II [38], AMASC [39], and the biological inspired joint stiffness control mechanism [40] and pneumatic muscles [41]. Another realization for stiffness altering is achieved through the principle of lever mechanism. This is accomplished by altering the distance between the pivot and the elastic element or output contact. Examples of this type include the AwAS [42], AwAS-II [43], CompAct-VSA [44], the vsaUT [45], the mVSA-UT [46], the vsaUT-II [47], the HDAU [48] and the pVSJ [49]. Further innovative methods that were used to vary the stiffness include altering the number of effective spring coils or "Jack Spring" [50], or altering the effective length of a leaf spring [51], [50]. The MACCEPA [52], MACCEPA 2.0 [53] and the DLR FSJ [54] which benefit from a nonlinear connector between the output link and the spring element to adjust the preload of the linear spring. Moreover, other techniques for stiffness variation is introduced. A recent method applies permanent magnets as method of stiffness variation [55].

A more recent approach to vary the stiffness was realized through discretely selecting the level of stiffness by adding/subtracting a number of elastic elements. The elastic elements are engaged through a locking mechanism or simply a clutch/brake., and they can either be arranged in series (the pDVSJ) [56], or in parallel. The realization of the latter is referred to as Series-Parallel Elastic Actuators [57].

The design of Series-Parallel Elastic Actuators (SPEA) was driven by the need to minimize energy consumption, peak torque, or power consumption in robots and humans [57]. This concept is introduced in the iSPEA [58]. In this actuator, the springs are connected to the output link

from one side and to an intermittent mechanism on the other side. This mechanism converts a continuous (rotational) input into two consecutive phases. This yields a succession of springs' involvement by altering the output torque of the actuator. MACCEPA-Based SPEA is another example of SPEA and is illustrated in [59], where the springs are recruited through a cylindrical cam mechanism. Another illustration is the +SPEA [60]. This actuator benefits from the parallel motors, locking mechanisms and springs to drastically reduce the energy requirement. The previously mentioned examples applied locking mechanism in recruiting springs. Clutches/Brakes were introduced to SEA in Clutched Serial Elastic Actuators towards energy consumption minimization [61]. This concept was extended in the SPEA in [62], where electro- adhesive clutches were integrated in a leg exoskeleton, providing both light-weight and energy efficiency. In this work, the concept of SPEA is being applied in other application (i.e. passive haptics).

In passive haptic interfaces, stiffness can be simulated through variable stiffness joints. This requires (a) a wide range of stiffness to be covered, (b) the capability to change the stiffness at any position without reverting to the initial equilibrium point, and (c) a swift change in the level of stiffness. This has motivated various studies and new designs of variable stiffness mechanisms with passive compliance for haptic applications, such as the pVSJ [49], and pDVSJ [56].

This paper presents, a novel passive variable stiffness joint as a bench-test for further development towards the above proposed haptic devices. The proof-of-concept design demonstrates the ability to vary the stiffness from transparency to high values through changing the number of the associated series-parallel elastic elements. The main contribution of the presented concept lies in its simplicity, scalability, and modularity (capability to involve an (n) number of series-parallel elastic elements to achieve (2^n) levels of stiffness. Moreover, the novel joint can rotate freely at the zero stiffness case without limits. Beside the modularity, the contributed design has the ability to directly select the involved elastic element(s) without the need of succession involvement used in the previously proposed designs in literature. The remainder of the manuscript is organized as follows: The concept and design are presented in section II. Stiffness modeling and the dynamic model are detailed in section III. While the physical implementation and experimental results are described in section IV. The psychophysical experiments are illustrated in section V. A discussion to illustrate a comparison between the presented design and the state-of-art designs in literature is presented in section VI. The limitations of the system is being discussed in section VII. Finally, the conclusions and future work are highlighted in section VIII.

II. CONCEPT AND MECHANICAL DESIGN

A. CONCEPT OF THE BPVSJ

The main inspiration behind the design of the *BpVSJ* is the series-parallel variable stiffness mechanism [58]–[60]. In this type of mechanisms, the stiffness is altered by changing the number of associated elastic elements. The elastic elements are parallel with respect to each other, and their combined stiffness is connected in series with a load (output link) at one end. The other end can be connected in series with a clutching mechanism and an actuator (motor) in an active system. On the other hand, the elastic elements in a passive system can be grounded through controllable locking mechanisms such as clutches/brakes. The new concept is demonstrated in Fig. 2. A brake is serially connected to a torsion spring and then a spur gear, which is then coupled to the main spur gear of the load shaft (Fig. 2a). The brake-torsion spring-gear unit is referred to as a *Stiffness Bit*, which provides the stiffness of the torsion spring to the main shaft of the load. By connecting n stiffness bits to the main spur gear of the load shaft in parallel, the sum of all the torsion springs' stiffness will be the output stiffness of the joint as in Fig. 2b. Theoretically, without considering overlapping stiffness results, there are $(n + 1)$ different possible stiffness combination. Here, the number 1 indicates the zero stiffness case, which facilitates the capability of unlimited motion of the output arm at the transparency where all brakes are inactive. In general to obtain 2^n levels of stiffness from n springs in parallel, any combination of stiffness values must be unique. Thus, for a system consisting of three springs, the stiffness of each spring K_x must follow the following conditions:

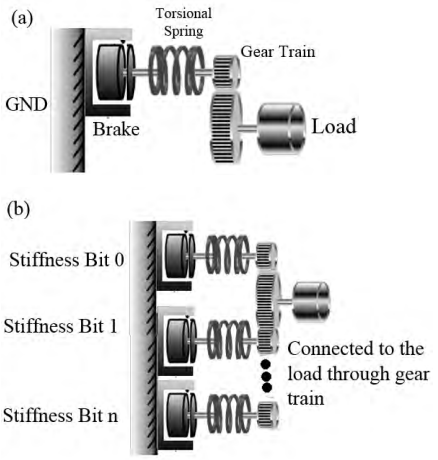

FIGURE 2. (a) Stiffness bit, the set of a grounded brake connected to an elastic element (spring) which would react against the load torque through the gear train. (b) Multiple stiffness bits connected to the output link (Load) through combined gear trains.

$$K_i \neq K_j \quad i \neq j,\ \{i, j \in \{0, 1, 2\} \tag{1}$$

$$K_i + K_j \neq K_k \quad i \neq j \neq k,\ \{i, j, k \in \{0, 1, 2\} \tag{2}$$

The key novelty of the BpVSJ lies in the design topology as depicted in Fig. 3. Three custom-made torsional springs with three different values (K_0, $2K_0$, $4K_0$), respectively, are connected to three brakes, forming three stiffness bits. The combination of stiffness values can be presented through a binary representation based on an active/inactive stiffness

TABLE 1. Achievable stiffness levels of BpVSJ.

Stiffness Bit 2^2 ($4K_0$)	Stiffness Bit 2^1 ($2K_0$)	Stiffness Bit 2^0 (K_0)	Stiffness Level
0	0	0	0
0	0	1	K_0
0	1	0	$2\ K_0$
0	1	1	$3\ K_0$
1	0	0	$4\ K_0$
1	0	1	$5\ K_0$
1	1	0	$6\ K_0$
1	1	1	$7\ K_0$

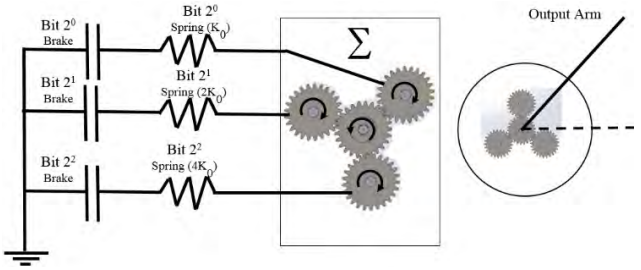

FIGURE 3. Concept of the BpVSJ; the stiffness is altered by changing number of involved springs.

bit. The other end of each spring is connected to a planet gear, which contributes partially to the resultant torque of the sun-gear that is connected to the output arm. An active stiffness bit applies torque on the output arm. If the stiffness bit is inactive, the spring will run-freely through a grounded bearing. This will facilitate the capability of unlimited motion of the output arm at the transparency (zero stiffness level) where all the brakes are inactive. The achievable stiffness levels in binary representation are shown in Table 1. An active stiffness bit is represented by ''1'', while an inactive stiffness-bit is represented by ''0''. Another advantage of this topology is the modularity or capability of altering the stiffness level at any joint deflection position with very low switching time. Lastly, the scalability can be achieved either by changing the value of K_0 or by adding extra Stiffness-Bits.

B. Mechanical Design of the BpVSJ

BpVSJ is designed as a passive haptic interface that is capable to simulate different levels of stiffness in virtual reality and remote environment applications. The desired maximum simulated angular stiffness is 3.5 N.m/degree. This value is selected based on literature to cover a wide spectrum of elastic elements [63], as three Stiffness-Bits are used to simulate seven levels of stiffness. The springs should have the stiffness levels of 0.5 N.m/degree, 1 N.m/degree, and 2 N.m/degree for the first, second and third stiffness-bit respectively.

Realization of the mechanical system of the BpVSJ can be seen in Fig. 4a. The lower base is fixed and consists of ten bearings that hold 10 shafts. Three of these shafts are connected to three electromagnetic friction brakes. Four shafts are used for the sun-planet gear train, forming a (1:1) ratio for

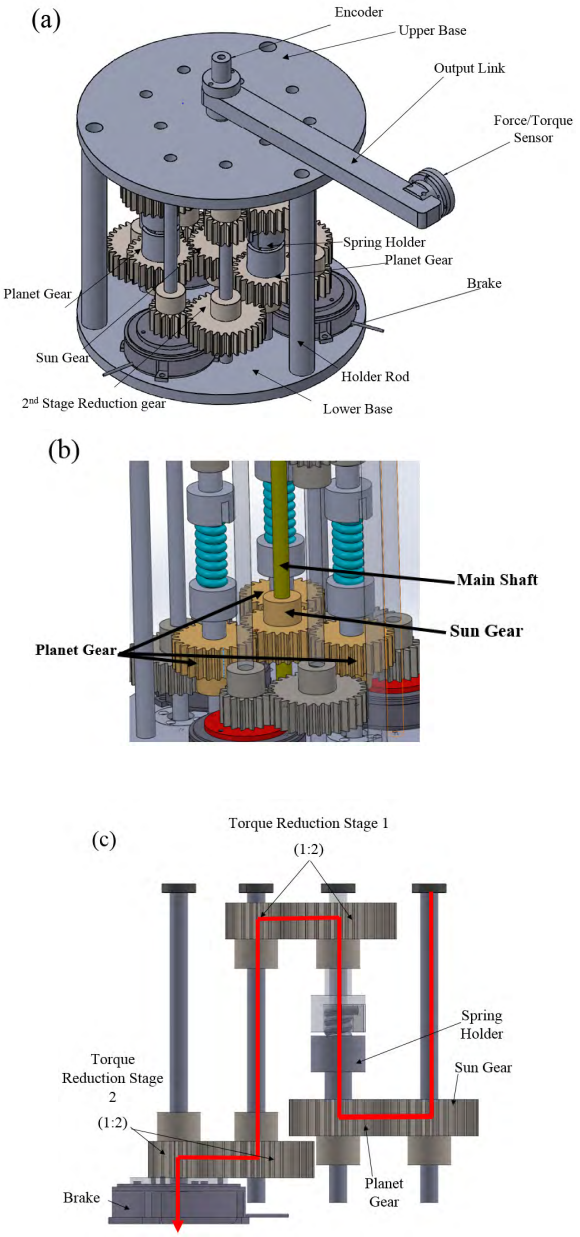

FIGURE 4. (a) The mechanical design of BpVSJ, (b) The sun planetary gears used in BpVSJ (c) Torque transmission path (red arrow) for each stiffness-bit. the torque reduction gear train is needed to keep the torque on the brakes lower than the maximum allowed ones without compensating the maximum desired external torque (21 N.m).

each planet: sun train (depicted as golden gears in Fig. 4b). The three planet gears hold three torsional springs (each gear holds one spring) from below through the spring holders.. The last three shafts are used for the two Torque Reduction Stages (TRS). The torque reduction stages are needed to maintain the torque exerted on the brakes lower than the maximum allowable torque of the brake without compromising the maximum desired external torque. These brakes were selected off-the-shelf with maximum torque to size ratio. If the brakes were stronger (with same size), the TRS can be opted. The torque

transmission path (red arrow) for each stiffness-bit is shown in Fig. 4c. The torque is transmitted from the user hand through the output link. The output link is connected to a sun gear which transmits the torque to the spring holder through the planetary gear. The torsional spring is connected to two spring holders, which are part of the shafts where the planetary gear and gear from TRS1 are mounted. The first torque reduction stage connects the upper end of the spring holder through 1:2 torque reduction ratio. The second stage of torque reduction (1:2) is transmitting the torque to the brake, resulting a (1:4) torque reduction in total. The arrangement of two stages is selected to minimize the diameters of the lower and upper bases. From the figure, it can be seen that if the brake is active, the output arm will deflect the spring and the user would feel the altered stiffness. If the brake is inactive, the gears will rotate freely and the user would feel no stiffness.

III. JOINT'S MODELING

A. STIFFNESS MODEL

Altering the stiffness of BpVSJ is achieved through changing the number of involved parallel elastic elements. The involvement of an elastic element is achieved through grounding one end of the spring via an electromagnetic brake. The stiffness model will be derived from the kinematics model of the joint illustrated in Fig 5.

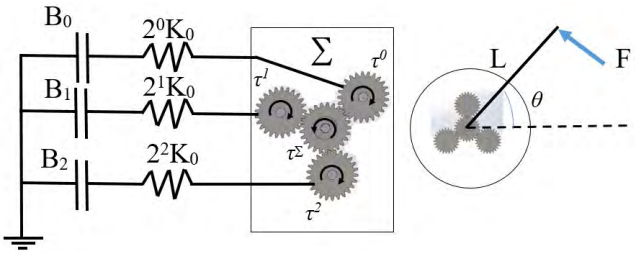

FIGURE 5. BpVSJ; stiffness model the K_0 is the base value for the springs, C1, C2, C3 represents brake 1,2,3 respectively. User's hand force (F) is applied on the output link with a length of (L).

A pushing force (F) exerted by the user's hand is creating a torque through the arm length (L). The resultant torque (τ^{Σ}) will rotate the main shaft with the sun gear. In the case where all stiffness-bits are inactive, the torque and motion will be transmitted freely through the planetary gears, into the torsional springs which they would rotate freely with no compression. In case of any active stiffness-bit(s), the motion of shaft connecting the end of the involved torsional spring to the brake will be blocked. In the presence of the exerted torque on the main shaft, the involved torsional springs will deflect, yielding a counter torque that would be felt as resistance force by the user's hand.

Deriving the stiffness model starting from the resultant torque (τ^{Σ}) equation as follows

$$\tau^{\Sigma} = \mathrm{F} \times \mathrm{L} = -(\tau^0 + \tau^1 + \tau^2) \tag{3}$$

where τ^0, τ^1, τ^2 are the torque of the stiffness bits 0, 1 and 2 respectively.

Each of these torques can be represented in the following equation:

$$\tau^{\mathrm{n}} = \beta_n \left(2^n (K_0) (\theta - \phi_n - \varphi)\right), \quad n \in \{0, 1, 2\} \tag{4}$$

$$\phi_n = \theta \left(t_{ON,n}\right), \quad n \in \{0, 1, 2\} \tag{5}$$

$$\beta_n = \begin{cases} 0, \text{ if Brake (n) is inactive} \\ 1, \text{ if Brake (n) is active} \end{cases} \tag{6}$$

where (β, θ, ϕ, φ), are the binary function, joint angular position at the current time, joint angular position at the activation time (t_{ON}), and the backlash angle, respectively. The joint stiffness is the rate of change of the torque with respect to the angular deflection.

From the previous equations, the rendered torque (τ^{Σ}) and the total stiffness (K_{Σ}) can be derived as follows:

$$\tau^{\Sigma} = \sum_0^n \beta_n \left(2^n (K_0) (\theta - \phi_n - \varphi)\right), \quad n \in \{0, 1, 2\} \tag{7}$$

$$K_{\Sigma} = \frac{\delta \tau^{\Sigma}}{\delta \theta} = \sum_0^n \beta_n (2^n (K_0)), \quad n \in \{0, 1, 2\} \tag{8}$$

From (5), it can be concluded that the involvement of each spring is independent from other spring. Hence, the level of stiffness can be altered at any position without the need of reverting to the initial equilibrium point. From (6), it can be concluded that the joint stiffness is dependent on the number of stiffness-bits (n) and the base stiffness value (K_0). This feature allows the scalability of the model in both the stiffness range and the realized number of stiffness values.

B. DYNAMIC MODEL

BpVSJ is a passive rotary single degree-of-freedom joint that is meant to be used as a passive haptic interface. For haptic interfaces, dynamic models are important to determine the system's bandwidth and the system's range of impedance [64]. The dynamic model of the system is assumed to be a simple Inertia-Damper-Spring system and it is written as follows:

$$I\ddot{\theta} + B\dot{\theta} + K\theta = \tau_h \tag{9}$$

Where I, B, K, τ_h, θ are the moment of inertia, damping coefficient (includes friction damping in gears and between moving parts), stiffness, input (hand) torque, and angular deflection respectively. The stiffness coefficient can be calculated through the stiffness model presented in the stiffness model section.

In order to estimate the inertia and damping coefficients, BpVSJ was subjected to a fixed input torque equalized by the spring tension. From this equilibrium state, BpVSJ is released and the angular position is recorded. Applying the Nonlinear Least Square Method (Using MATLAB SIMULINK parameters estimation toolbox), all dynamic parameters were estimated empirically. Although the results of least square method are not unique, but it doesn't affect the purpose of the identification. As the identification results are enhanced through taking several samples and calculating the mean and the variance for these samples. Table 2 illustrates the

TABLE 2. Dynamics system coefficients for BpVSJ.

Parameter	Estimated Value	Unit
I	0.062±0.02	Kg.m2
B	1.1±0.24	N.m.s/rad

estimated parameters theoretically and empirically. From the results, it can be concluded that for a system with low speed and acceleration the effect inertia and damping effects will be very low compared to the stiffness coefficient. The bode plot for the system is illustrated in Fig. 6. It can be concluded from the figure that the bandwidth of the system is relatively low and can hence be used for some applications, like haptic exploration tasks [34], [65].

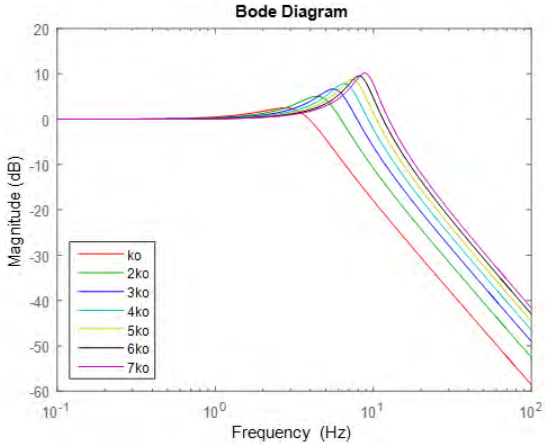

FIGURE 6. The bode plot for BpVSJ for all stiffness levels, it can be seen that the bandwidth of the system is dependent on the level of stiffness levels from 1 to 7 and it has the values of {4.7 Hz, 7 Hz, 8.83 Hz, 10.3 Hz, 11.6 Hz, 12.8 Hz, 13.8 Hz} respectively. From these values, it can be concluded that BpVSJ is suitable to be used as haptic interface for exploration applications.

The damping coefficient (B) represents the general friction in the system. Friction occur mainly between the gears during transmission. The damping coefficient effects the minimum rendered torque at the zero-stiffness level. For BpVSJ, the minimum rendered torque at zero stiffness level was approximately 1.2 N.m @ 1 rad/s angular velocity. It's worth to mention that the Coulomb friction is neglected due to the purpose of dynamic modeling.

IV. IMPLEMENTATION OF THE BPVSJ

The dynamic structure of the BpVSJ consists of ten Stainless Steel A316 shafts (Diameter: 10 mm). The spring capsules were machined as a part of the shafts to eliminate any undesirable slippage. The three torsional springs are made of Stainless Steel A316 (detailed design parameters can be found in Table 3, where S0, S1, S2 indicate the springs used in Stiffness Bit 2^0, 2^1, and 2^2, respectively). The springs were calibrated to determine their linear range which is presented in Fig. 7. It is worth to mention that the deviation in S2's behavior can be due to the human fabrication error as the

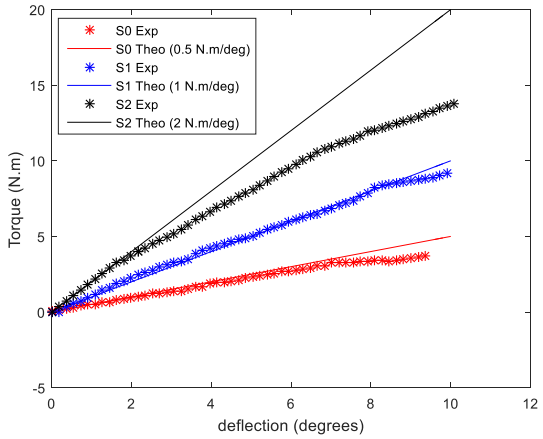

FIGURE 7. Torque vs Deflection of the three springs (S0, S1 and S2).

TABLE 3. Torisonal springs parameters.

Parameters	S0	S1	S2	Unit
Diameter of Spring Wire	5	6	8	(mm)
Outer Diameter	16.8	18.25	24.2	(mm)
Inner Diameter	6.8	6.25	8.2	(mm)
Number of Active coils	5.25	5.25	6.25	
Linear Range (Safe Travel)	7.7	9	2.1	degrees

springs were fabricated in lab. The sun and the three planetary gears are (Misumi GEAHBB2.0-25-20-B-10, 25 teeth). The two (2:1) torque reduction stages are composed of six gears (Misumi GEAHBB2.0-30-20-B-10, 30 teeth) and another six gears (Misumi GEAHBB2.0-15-20-B-10, 15 teeth). The static structure consists of the upper base, lower base and two radial bearing bases made of Aluminum. These bases encapsulate ball bearings to hold the shafts and prevent any buckling due to the shear bending caused by the contact forces of the blocked gears. The base holders are made of Stainless Steel rods (Diameter: 12 mm) and the output link is made of an Aluminum Alloy (300 mm in length).

The sensory system of the BpVSJ includes a force/torque sensor (ATI Mini 40) mounted on the forearm to measure the torque on the output link, a quadrature rotary encoder (RS-260-3768) mounted on the main shaft to measure the output link's deflection (θ), a National Instrument DAQ (NI-USB-6343), and National Instrument LabVIEW® for real time control and data acquisition (rate of 1000 samples per second). The stiffness bits are activated through the grounded brakes (Mayr 3/520-212.01/24), which are powered by 2-series connected 12 VDC batteries and controlled through Arduino 4-channel Relay Module by the DAQ.

Experiments were conducted to validate the stiffness model. The characterization test was performed on a horizontal vice (Fig. 8) to eliminate any gravitational potential energy effect. As springs S0 and S1 have a wider linear range than S2. Their individual stiffness levels (level 1 and 2) and combined

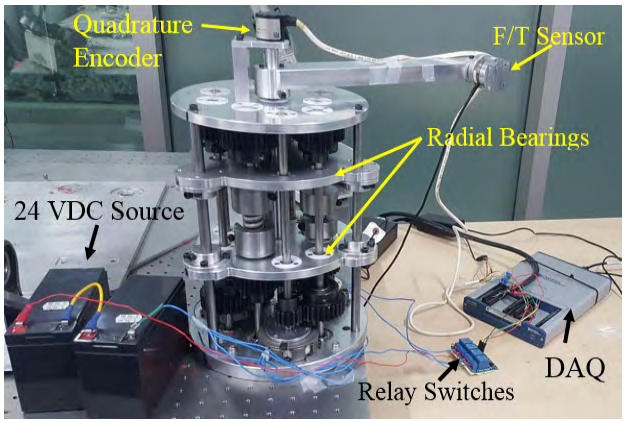

FIGURE 8. The test bed of BpVSJ , the joint is mounted on a horizontal plane table to eliminate the effect of gravitational energy.

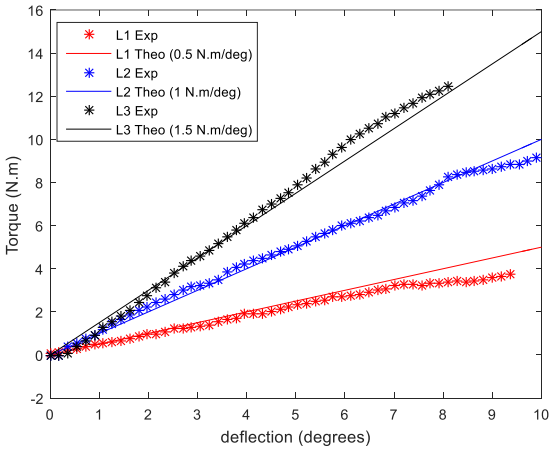

FIGURE 9. Evaluating stiffness levels (level 1 (red), level 2 (blue) and level 3 (black)). The experimental results has proven that the system works for the proposed model at levels 1,2, and 3. the error can be referred to exceeding the safe travel at deflection 7 degrees for L1, and 9 degrees for L2. The error in L3 can be referred to the different resolutions of F/T sensor and the encoder (Error in stiffness between theoretical and experimental L1: 12.1%, L2: 2.5%, L3: 10.9%).

stiffness level (level 3) are shown in Fig 10. For the stiffness levels where S2 were involved (level 4, 5, 6 and 7), the linear range is limited to 2 degrees and shown in Fig. 11. It can be seen from both figures that the model is verified in the linear ranges of the springs. The sources of errors can be referred for exceeding the safe travel regions of the springs. As the springs were fabricated in the lab, a slight error in the actual stiffness of the springs is present compared with the desired stiffness (S0: 12.1 %, S1: 2.5%, and S2: 3%). Another source of error can be referred to human error and the different resolutions of the F/T sensor and the encoder (one order of magnitude). As BpVSJ is meant to render stiffness levels, the error will not affect the functionality of the device as a haptic interface for stiffness rendering. Further discussions is illustrated in section V, where the system is validated through psychophysical experiments.

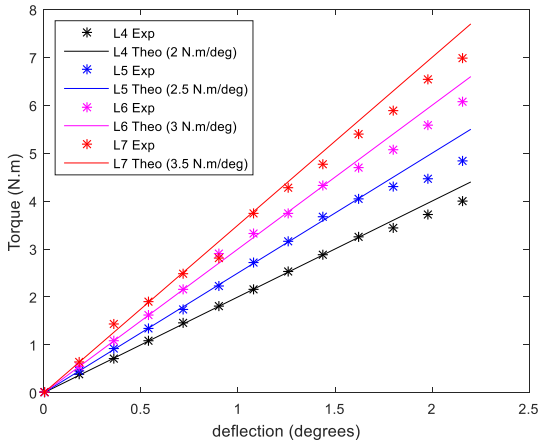

FIGURE 10. Evaluating stiffness levels (level 4 (black), level 5 (blue) levles 6 (pink) and level 7 (red)) the experimental results has proven that the system works for the proposed model at levels 4, 5, 6, and 7. The error can be referred to the different resolutions of F/T sensor and the encoder (Error in stiffness between theoretical and experimental: L4:3% L5: 8.3%, L6: 6.8%, L7: 8.3%).

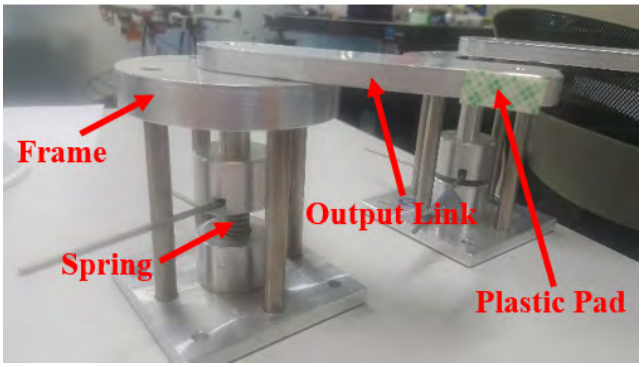

FIGURE 11. Stiffness mimic devices with calibrated springs.

The power consumption of the system depends on the number of active stiffness bits. A single stiffness bit power rate is typically 15 W. Hence, the power consumption can range between 15 to 45 W. It is noteworthy here that the stiffness variation time is same as the on-time of the brake which is 35 ms. Comparing the stiffness variation time of BpVSJ (35 ms) as an example of Discrete Variable Stiffness Actuator to DLR FSJ [54] (300 ms) as an example of continuous variable stiffness actuators, it can be seen that the BpVSJ is one order of magnitude faster than DLR FSJ [54]. This has been achieved with the sacrifice of the continuous stiffness range that continuous variable stiffness actuators like DLR FSJ can achieve. Comparing with the power consumption of BpVSJ (Max: 45 W) to pDVSJ-II [66] (Max. 122.4W) as another example of discrete variable stiffness actuators, it can be seen that BpVSJ has a better power efficiency compared to its counterpart. The power consumption can be minimized through developing lower power consuming brakes, such as MRI based brakes. The design and power parameters of the BpVSJ are illustrated in tables 4 and 5.

V. HAPTIC INTERFACES & THE PSYCHOPHYSICAL TEST

In order to measure the capability of the BpVSJ to display different levels of stiffness that are cognitively realized by

TABLE 4. System design parameters.

Specification	Value	Unit
Lower Base Diameter	230	mm
Upper Base Diamter	220	mm
Output Link Length	300	mm
Main Shaft Length	305	mm
Other Shafts Length	287	mm
All Shaft's diameter	10	mm
Total BpVSJ Length	348	mm
Gross Weight	17.9	kg

TABLE 5. System's power and sensor's specfications.

Specification	Value	Unit
Encoder Resolution	0.18	degrees
Force/ Torque Sensor Force Resolution	0.01	N
Sampling Rate	1000	Hz
Single brake Power Rate	15	W
Maximum Power Rate	45	W
Stiffness Switching time	35	ms

users, two tasks as part of a psychophysical experiment were performed on volunteer participants. The experimental protocol is similar to [65]. The tasks were designed to be totally passive, where only active-push cognitive tasks were be performed: the Relative Cognitive Task and Absolute Cognitive Task [65]. In this section, the participants' selection criteria, the experimental design and setup, detailed procedures, as well as the experimental results are detailed.

A. EXPERIMENTAL SETUP

Three mimic devices were fabricated, each consisting of an output link, and a torsional spring. The stiffness value of each spring is similar to one of the values rendered by BpVSJ (see Fig. 12). The springs were selected to approximately represent levels L1, L3 and L5 of the BpVSJ. The detailed design parameters of the springs are shown in Table 6. Hereinafter, the mimic device with the springs with highest stiffness, intermediate stiffness, low stiffness will be labeled as SH, SM and SL, respectively. The rendered levels in the BpVSJ (levels L1, L3 and L5) will be denoted as L, M, and H, respectively.

TABLE 6. Springs parameters for the stiffness mimic devices.

Parameter	SH	SM	SL	Unit
Torsional Stiffness	2518.6	1513	496.5	N.mm/deg
Wire Diameter	8	7	5	mm
Outer Diameter	27	22	15	mm
Number of Active Coils	4.25	5.25	6.25	Coils
Material	Stainless Steel A316 Alloy			

The tips of the output links of SH, SM, SL and the BpVSJ were covered with 1 mm plastic pads in order to minimize perception bias in terms of the material softness or temperature.

B. PARTICIPANTS

20 right-handed healthy participants (9 Females, 11 Males, Age: 30.5 ± 3.74) gave their informed consent to participate in the two task experiment. Exclusion criteria consisted of any upper-body physical limitations, disease or movement dysfunction that may affect the experimental outcomes. The experimental procedure was approved by the Ethics Committee of Healthpoint Hospital -- Abu Dhabi -- United Arab Emirates (Ref. REC006).

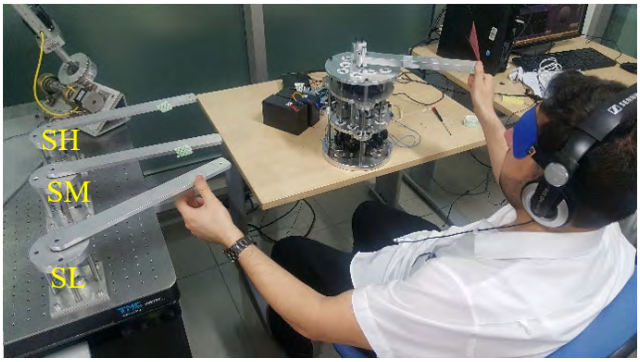

FIGURE 12. Participant performing the absolute cognitive task.

C. ACTIVE RELATIVE COGNITIVE TASK

During this task, the participants were guided to use the tip of their thumb to probe and sort three levels of stiffness as rendered by the BpVSJ. More specifically, the participants were presented with 5 different sets of stiffness. Each set included 3 stiffness levels randomly displayed that the participants were asked to rank from the lowest to the highest stiffness. During the experiment, the participants were seated on a chair, blind-folded and were exposed to an acoustic white-noise in order to prevent any auditory or optic cue. They were granted unlimited time to perform the task, and guided to push the stylus of the BpVSJ using the thumb of the dominant hand until the stylus deflected by 5-10 degrees. It's worth to mention, that even BpVSJ is not following the linear behavior of stiffness level 5 when the deflection exceeds 2 degrees, the torque and stiffness is relatively higher than previous stiffness levels. Thus, the user will still feel higher stiffness. The results are shown in Table 7, where the perception of the stiffness displayed by the BpVSJ was associated with the perception of the real values in a confusion matrix. The diagonal of the matrix represents the right answers.

TABLE 7. Confusion matrix of relative cogitive task.

Displayed \ Real	H	M	L	Relative Accuracy
H	96	4	0	96
M	0	97	3	97
L	0	1	99	99

D. ACTIVE ABSOLUTE COGNITIVE TASK

In this task, participants were guided to use the tip of their thumb to probe three levels of stiffness as rendered by the BpVSJ and relate them to their physical counterparts displayed on the mimic devices. The participants were presented with the randomly displayed stiffness levels. Each of the three levels were randomly displayed 5 times. The participants

needed to associate the rendered stiffness with its physical counterpart using their left hand. During this task, the participants were also seated on a chair, blind-folded and exposed to an acoustic white-noise in order to prevent any auditory or optic cue. They were granted unlimited time to perform their task and guided to push the stylus of the BpVSJ by the right thumb and the stylus of the mimic device by the left thumb, such as either stylus would deflect 5-10 degrees (Fig. 13). The results are depicted in Table 8, where the perception of the stiffness displayed by the BpVSJ was associated with the perception of the real values in the mimic devices in a confusion matrix. The diagonal of the matrix represents the right answers. The errors of the absolute cognitive tasks may be explained by the laterality of the participants and the fact that the mimic devices have less friction compared to BpVSJ as the mimic devices have no gears.

TABLE 8. Confusion matrix of absolute cogitive task.

Displayed \ Real	SH	SM	SL	Relative Accuracy
H	74	26	0	74
M	7	77	16	77
L	0	2	98	98

E. RESULTS DISCUSSION

Two psychophysical experiments were conducted with 20 healthy participants. These experiments are the Relative Cognitive Tasks (RCT) and the Absolute Cognitive Tasks (ACT). These experiments are well-established in literature [64], [65] to validate the capability of a haptic interface to render a physical stimuli (stiffness for this case) and being recognized by the users. In the RCT, the users will feel different levels of stiffness rendered by the haptic interface and they're requested to order these levels from highest to lowest. While in ACT, the users will feel different levels of stiffness from the haptic interface and they are requested to match it with their calibrated counterparts on a mimic device.

The results of conducting such experiments are plugged in a confusion matrix, which relates the stiffness level recognized by the users to the actual stiffness value they felt. If the user recognized the actual stiffness level, it is considered a right answer. If the user confused the actual level of stiffness with another value then it is considered a wrong answer. The percentage of the right answers reflects the relative accuracy of recognizing this particular level of stiffness. The average of the relative accuracies reflects the capability of the haptic interface of rendering different levels of stiffness and verify it to be used by humans.

Comparing the results of BpVSJ with the validated haptic interfaces proposed and [64] and [65], The results show that the users have recognized the levels of stiffness rendered by the BpVSJ with an average of 97% for the Relative Cognitive Task, and 83% for Absolute Cognitive Task. In [65], similar experiments were conducted on the validated haptic interface and the results of the Relative Cognitive Task is 91% and Absolute Cognitive Task is 82%. While in [64], only Relative Cognitive Task is conducted to validate the proposed device and the results are an average of 70%. From this, it can be concluded that BpVSJ is verified as haptic interfaces.

VI. DISCUSSION

The design of BpVSJ goes under the category of Series-Parallel Elastic Actuators (SPEA). This designs proposed in this category were driven by the need to minimize energy consumption, peak torque, or power consumption in robots and humans [57].

In literature, several concepts of SPEAs were presented. The iSPEA [58] and the MACCEPA-Based SPEA [59] are two examples of SPEAs which benefit from an intermittent mechanism to recruit the parallel elastic elements in succession. While BpVSJ benefits from the gear train formation and the brakes to allow the freedom in selecting the level of stiffness without the need of succession involvement of elastic elements. Similar to BpVSJ, the work in [62] used electro-adhesive clutches to control the engagement of the elastic elements. The electro-adhesive clutches are well-known for their low power consumption, but the design in [62] still applies succession in elastic element involvement, which limits the freedom of selecting the level of stiffness at any desired position.

Although the current proof-of-concept is relatively large, the concept of the design allows the designer to realize more compact versions. The current bulkiness is referred to the fact that all the used parts were off-the shelf. The problem can be avoided by selecting stronger brakes, which will omit the need of the torque reduction gear stages. Compared to the previous proposed designs, BpVSJ has relatively fast response time with relatively low power consumption.

Passive haptic interfaces that involves variable stiffness mechanisms are found in literature in [34], [56], and [66]. BpVSJ is able to achieve zero stiffness level, enabling its application in teleoperation applications, while in [34] the device covers a large span of stiffness levels benefitting from the concept of Variable Lever Mechanism (VLM) but is not able to achieve zero stiffness. The design proposed in [34] is quite bulky and the system is not easily scalable to be embedded in a revolute joint, while the design of BpVSJ is scalable and can be embedded in a revolute joint enabling it to be integrated with multiple-degrees-of-freedom haptic interfaces. The concept altering the stiffness in pDVSJ [56] and pDVSJ-II [66] relies on changing the active length of an elastic cord [56] or the number of involved springs-in-series [66]. This was achieved through activating the novel selective-locking mechanism (Cord Grounding Unit (CGU)) which limits the motion of the free cord creating a new active length [56] or involve the desired number of springs [66]. In these designs, a single level of stiffness requires two springs (one spring per direction) yielding 0.5n levels of stiffness for n springs. While in BpVSJ, there are 2^n levels of stiffness for n springs. On the same hand, the devices presented in [56] and [66] is capable to change the stiffness from lower-stiffness to higher stiffness due to the usage of

CGUs, while in BpVSJ, the user is capable to change freely from lower levels to higher levels and visa-versa.

VII. LIMITATIONS

As BpVSJ belongs to the category of passive haptic interfaces, it inherits the limitations of all passive haptic interfaces in their inability to generate a force that will change the direction of motion of the user's hand. This fact prevents passive haptic interfaces to be used in several applications like bilateral teleoperation with obstacle avoidance through artificial force fields [67]. Moreover, the system lacks controllable energy dissipative elements (i.e brakes), the system is incapable to control its damping coefficients preventing it from being used in haptic applications where motion redirecting is required (i.e. path following [68]

BpVSJ is designed to fully simulate the interaction of elastic elements without sacrificing the natural passivity of its system. The designated applications where BpVSJ can used is limited to exploration where remote object stiffness rendering is required. An example of such applications can be found in [66] where the passive haptic interface (BpVSJ in this case) can be used as a master device to teleoperated a remote slave manipulator that explores and inspects different remote objects by pressing on them (performing palpation). The stiffness is rendered on the haptic interface based on the force gradient transmitted through the bilateral teleoperation system. In case the virtual/remote elastic object has a fixed value stiffness, only one level of stiffness in BpVSJ will be activated during the interaction. While in case the remote/virtual object has a nonlinear stiffness, the level of stiffness in BpVSJ may change higher or lower based on the change in the behavior of the object's stiffness.

The BpVSJ is meant to be used in exploration application where the joint will be moving freely till there is an interaction with an elastic element. Its supposed to change the stiffness from zero stiffness to the designated level. In our approach the objective is to discretely change the level of stiffness which is obliviously less smooth than altering the stiffness of an active haptic interface, but has advantages in terms of speed of stiffness variation, and minimizing energy consumption which is the main motivation for the design topology. Moving towards multiple-Degrees-of-freedom haptic interface that incorporates the concept BpVSJ is achievable. The stiffness of the end-effector will be dependent on both joints stiffnesses and joints position. It can be speculated that the system will be less smooth than an active haptic interface.

VIII. CONCLUSIONS AND FUTURE WORK

This paper presented the BpVSJ as a proof of concept of a novel passive revolute joint that is able to vary its stiffness by leveraging the recruitment of Serial-Parallel Elastic Elements. The novelty of the system lies in its design topology, where three torsional springs are mounted on three planet gears on one side. The planet gears are directly connected to a sun gear mounted on the main shaft. The other side of the each spring is mounted on a brake through two torque reduction gear trains. The joint has shown unlimited motion of the output arm at the transparency level (zero stiffness where all brakes are inactive), and seven different stiffness levels based on combinations of active stiffness bits. The BpVSJ has demonstrated the capability of altering the stiffness at any joint angular position, where the recruitment of a particular stiffness level can occur at a non-equilibrium point without additional power. The theoretical stiffness model was experimentally validated, demonstrating that the stiffness can be altered on the linear ranges of the torsional springs.

To test the capability of the BpVSJ as a functional passive haptic interface for stiffness rendering, a psychophysiological experimental test was conducted with volunteer participants. The participants conducted two tasks: a relative cognitive task and an absolute cognitive task. The results confirmed that the BpVSJ is capable of rendering stiffness with high relative accuracy.

The simplicity of the BpVSJ design facilitates relative compactness and scalability of future versions. For wearable haptic interface, the current proof-of-concept realization suffers from bulkiness. The authors recommend applying dog clutches or tooth clutches for high torque to size ratio. This would allow for a more compact system without compromising the designated torque rates. Torsional plate springs would also potentially contribute to a more compact design. BpVSJ suffers from the friction by the gear trains, in order to reduce the friction and maintain the passivity of the system, the authors suggest to change the gear trains with a pulley-driven system.

ACKNOWLEDGMENT

The authors would like to thank Dr. Nader Darwich, Chief of Orthopedics, and the Ethics Committee at HealthPoint Hospital for approving and facilitating the psychophysiological human experiments.

REFERENCES

[1] O. Hayward, O. R. Astley, M. Cruz-Hernandez, D. Grant, and G. Robles-De-La-Torre, "Haptic interfaces and devices," *Sensor Rev.*, vol. 24, pp. 16–29, Nov. 2004.
[2] D. Prattichizzo, C. Pacchierotti, and G. Rosati, "Cutaneous force feedback as a sensory subtraction technique in haptics," *IEEE Trans. Haptics*, vol. 5, no. 4, pp. 289–300, 4th Quart., 2012.
[3] C. Pacchierotti, G. Salvietti, I. Hussain, L. Meli, and D. Prattichizzo, "The hRing: A wearable haptic device to avoid occlusions in hand tracking," in *Proc. IEEE Haptics Symp.*, Apr. 2016, pp. 134–139.
[4] C. Pacchierotti, *Cutaneous Haptic Feedback in Robotic Teleoperation* (Springer Series on Touch and Haptic Systems). Cham, Switzerland: Springer, 2015.
[5] S. Lee, G. S. Sukhatme, G. J. Kim, and C.-M. Park, "Haptic control of a mobile robot: A user study," presented at the IEEE/RSJ Int. Conf. Intell. Robots Syst., Lausanne, Switzerland, Sep./Oct. 2002.
[6] S. K. Cho, H. Z. Jin, J. M. Lee, and B. Yao, "Teleoperation of a mobile robot using a force-reflection joystick with sensing mechanism of rotating magnetic field," *IEEE/ASME Trans. Mechatronics*, vol. 15, no. 1, pp. 17–26, Feb. 2010.
[7] L. M. Crespo and D. J. Reinkensmeyer, "Haptic guidance can enhance motor learning of a steering task," *J. Motor Behav.*, vol. 40, no. 6, pp. 545–557, 2008.
[8] X. Chen and S. K. Agrawal, "Assisting versus repelling force-feedback for learning of a line following task in a wheelchair," *IEEE Trans. Neural Syst. Rehabil. Eng.*, vol. 21, no. 6, pp. 959–968, Nov. 2013.

[9] T. R. Coles, D. Meglan, and N. W. John, "The role of haptics in medical training simulators: A survey of the state of the art," *IEEE Trans. Haptics*, vol. 4, no. 1, pp. 51–66, Jan./Mar. 2011.

[10] M. Ferre, I. Galiana, R. Wirz, and N. Tuttle, "Haptic device for capturing and simulating hand manipulation rehabilitation," *IEEE/ASME Trans. Mechatronics*, vol. 16, no. 5, pp. 808–815, Oct. 2011.

[11] F. Gosselin, C. Bidard, and J. Brisset, "Design of a high fidelity haptic device for telesurgery," in *Proc. IEEE Int. Conf. Robot. Autom.*, Apr. 2005, pp. 205–210.

[12] X. Wang and P. X. Liu, "Improvement of haptic feedback fidelity for telesurgical applications," *Electron. Lett.*, vol. 42, no. 6, pp. 327–329, Mar. 2006.

[13] Z. Ni, A. Bolopion, J. Agnus, R. Benosman, and S. Regnier, "Asynchronous event-based visual shape tracking for stable haptic feedback in microrobotics," *IEEE Trans. Robot.*, vol. 28, no. 5, pp. 1081–1089, Oct. 2012.

[14] A. Bolopion and S. Regnier, "A review of haptic feedback teleoperation systems for micromanipulation and microassembly," *IEEE Trans. Autom. Sci. Eng.*, vol. 10, no. 3, pp. 496–502, Jul. 2013.

[15] M. Maisto, C. Pacchierotti, F. Chinello, G. Salvietti, A. De Luca, and D. Prattichizzo. "Evaluation of wearable haptic systems for the fingers in Augmented Reality applications," *IEEE Trans. Haptics*, vol. 10, no. 4, pp. 511–522, Oct./Dec 2017.

[16] J. B. F. van Erp, "Guidelines for the use of vibro-tactile displays in human computer interaction," in *Proc. Eurohaptics*, 2002, pp. 18–22.

[17] A. Tobergte *et al.*, "The sigma.7 haptic interface for MiroSurge: A new bi-manual surgical console," in *Proc. IEEE Int. Conf. Intell. Robots Syst.*, San Francisco, CA, USA, Sep. 2011, pp. 3023–3030.

[18] *CyberGlove User's Guide*, IMMERSION Corp. San Jose, CA, USA, 2007. [Online]. Available: http://www.immersion.com/3d/docs/CGIIManual.pdf

[19] J. K. Salisbury and M. A. Srinivasan, "The proceedings of the first PHANToM user's group workshop," Massachusetts Inst. Technol., Cambridge, MA, USA, Tech. Rep. AITR-1596, 1996.

[20] A. Gupta and M. K. O'Malley, "Design of a haptic arm exoskeleton for training and rehabilitation," *IEEE/ASME Trans. Mechatronics*, vol. 11, no. 3, pp. 280–289, Jun. 2006.

[21] M. Turner, D. H. Gomez, M. Tremblay, and M. Cutkosky, "Preliminary tests of an arm-grounded haptic feedback device in telemanipulation," in *Proc. ASME Dyn. Syst. Control Division*, vol. 64, 1998, pp. 145–149.

[22] Z. Ma and P. Ben-Tzvi, "RML glove—An exoskeleton glove mechanism with haptics feedback," *IEEE/ASME Trans. Mechatronics*, vol. 20, no. 2, pp. 641–652, Apr. 2015.

[23] D. K. Swanson, "Implementation of arbitrary path constraints using dissipative passive haptic displays," Ph.D. dissertation, School Mech. Eng., Georgia Inst. Technol., Atlanta, GA, USA, 2002.

[24] C. Rossa, J. Lozada, and A. Micaelli, "Design and control of a dual unidirectional brake hybrid actuation system for haptic devices," *IEEE Trans. Haptics*, vol. 7, no. 4, pp. 442–453, Oct./Dec. 2014.

[25] W. J. Book, R. Charles, H. Davis, M. Gomes, and K. Danai, "The concept and implementation of a passive trajectory enhancing robot," in *Proc. ASME Dyn. Syst. Control Division*, Atlanta, GA, USA, 1996, pp. 633–638.

[26] M. Sakaguchi and J. Furusho, "Development of 2 DOF force display system using ER actuators," in *Proc. IEEE/ASME Conf. Adv. Intell. Mechatronics*, Atlanta, GA, USA, Sep. 1999, pp. 707–712.

[27] Y. Tenzer, B. L. Davies, and F. R. Y. Baena, "Programmable differential brake for passive haptics," *Robot. Auton. Syst.*, vol. 58, no. 3, pp. 249–255, 2010.

[28] A. H. C. Gosline and V. Hayward, "Eddy current brakes for haptic interfaces: Design, identification, and control," *IEEE/ASME Trans. Mechatronics*, vol. 13, no. 6, pp. 669–677, Dec. 2008.

[29] Y.-J. Nam and M.-K. Park, "A hybrid haptic device for wide-ranged force reflection and improved transparency," in *Proc. Int. Conf. Control, Automat. Syst.* 2007, pp. 1015–1020.

[30] D. Senkal and E. I. Konukseven, "Passive haptic interface with mr-brakes for dental implant surgery," *Presence*, vol. 20, no. 3, pp. 207–222, 2011.

[31] C. Cho, M. Kim, and J. B. Song, "Direct control of a passive haptic device based on passive force manipulability ellipsoid analysis," *Int. J. Control, Autom., Syst.*, vol. 2, no. 2, pp. 238–246, Jun. 2004.

[32] M. Achibet *et al.*, "Elastic-Arm: Human-scale passive haptic feedback for augmenting interaction and perception in virtual environments," in *Proc. IEEE Conf. Virtual Reality (VR)*, Mar. 2015, pp. 63–68.

[33] M. Bianchi, E. P. Scilingo, A. Serio, and A. Bicchi, "A new softness display based on bi-elastic fabric," in *Proc. 3rd Joint Eurohaptics Conf. Symp. Haptic Interfaces Virtual Environ. Teleoperator Syst.*, 2009, pp. 382–393.

[34] A. Song, D. Morris, J. E. Colgate, and M. A. Peshkin, "Real time stiffness display interface device for perception of virtual soft object," in *Proc. IEEE/RSJ Int. Conf. Intell. Robots Syst. (IROS)*, Aug. 2005, pp. 139–143.

[35] E. Basafa, M. Sheikholeslami, A. Mirbagheri, F. Farahmand, and G. R. Vossoughi, "Design and implementation of series elastic actuators for a haptic laparoscopic device," in *Proc. IEEE Annu. Int. Conf. (EMBS)*, Sep. 2009, pp. 6054–6057.

[36] D. Gan, N. G. Tsagarakis, J. S. Dai, D. G. Caldwell, and L. Seneviratne, "Stiffness design for a spatial three degrees of freedom serial compliant manipulator based on impact configuration decomposition," *ASME J. Mech. Robot.*, vol. 5, no. 1, pp. 011002-1–011002-10, 2013.

[37] G. Tonietti, R. Schiavi, and A. Bicchi, "Design and control of a variable stiffness actuator for safe and fast physical human/robot interaction," in *Proc. Int. Conf. Robot. Automat.*, 2005, pp. 526–531.

[38] R. Schiavi, G. Grioli, S. Sen, and A. Bicchi, "VSA-II: A novel prototype of variable stiffness actuator for safe and performing robots interacting with humans," in *Proc. IEEE Int. Conf. Robot. Autom. (ICRA)*, May 2008, pp. 2171–2176.

[39] J. W. Hurst, J. E. Chestnutt, and A. A. Rizzi, "The actuator with mechanically adjustable series compliance," *IEEE Trans. Robot.*, vol. 26, no. 4, pp. 597–606, Aug. 2010.

[40] S. A. Migliore, E. A. Brown, and S. P. DeWeerth, "Biologically inspired joint stiffness control," in *Proc. IEEE Int. Conf. Robot. Automat. (ICRA)*, Apr. 2005, pp. 4519–4524.

[41] B. Ugurlu, P. Forni, C. Doppmann, and J. Morimoto, "Torque and variable stiffness control for antagonistically driven pneumatic muscle actuators via a stable force feedback controller," in *Proc. IEEE/RSJ Int. Conf. Intell. Robots Syst. (IROS)*, Hamburg, Germany, Sep./Oct. 2015, pp. 1633–1639.

[42] A. Jafari, N. G. Tsagarakis, B. Vanderborght, and D. G. Caldwell, "A novel actuator with adjustable stiffness (AwAS)," in *Proc. IEEE/RSJ Int. Conf. Intell. Robots Syst. (IROS)*, Oct. 2010, pp. 4201–4206.

[43] A. Jafari, N. G. Tsagarakis, and D. G. Caldwell, "AwAS-II: A new actuator with adjustable stiffness based on the novel principle of adaptable pivot point and variable lever ratio," in *Proc. IEEE Int. Conf. Robot. Autom.*, May 2011, pp. 4638–4643.

[44] N. G. Tsagarakis, I. Sardellitti, and D. G. Caldwell, "A new variable stiffness actuator (CompAct-VSA): Design and modelling," in *Proc. IEEE/RSJ Int. Conf. Intell. Robots Syst.*, Sep. 2011, pp. 378–383.

[45] L. C. Visser, R. Carloni, and S. Stramigioli, "Energy-efficient variable stiffness actuators," *IEEE Trans. Robot.*, vol. 27, no. 5, pp. 865–875, Oct. 2011.

[46] M. Fumagalli, E. Barrett, S. Stramigioli, and R. Carloni, "The mVSA-UT: A miniaturized differential mechanism for a continuous rotational variable stiffness actuator," in *Proc. IEEE/EMBS Int. Conf. Biomed. Robot. Biomechatron.*, Jun. 2012, pp. 1943–1948.

[47] S. S. Groothuis, G. Rusticelli, A. Zucchelli, S. Stramigioli, and R. Carloni, "The variable stiffness actuator vsaUT-II: Mechanical design, modeling, and identification," *IEEE/ASME Trans. Mechatronics*, vol. 19, no. 2, pp. 589–597, Apr. 2014.

[48] B.-S. Kim and J.-B. Song, "Hybrid dual actuator unit: A design of a variable stiffness actuator based on an adjustable moment arm mechanism," in *Proc. IEEE Int. Conf. Robot. Autom.*, May 2010, pp. 1655–1660.

[49] M. I. Awad, "Modeling, design & characterization of a novel passive variable stiffness joint (pVSJ)," in *Proc. IEEE Int. Conf. Intell. Robot. Syst. (IROS)*, Oct. 2016, pp. 323–329.

[50] K. W. Hollander, T. G. Sugar, and D. E. Herring, "Adjustable robotic tendon using a 'Jack Spring,'" in *Proc. Int. Conf. Rehabil. Robot.*, Jun./Jul. 2005, pp. 113–118.

[51] J. Choi, S. Hong, W. Lee, and S. Kang, "A variable stiffness joint using leaf springs for robot manipulators," in *Proc. IEEE Int. Conf. Robot. Autom.*, May 2009, pp. 4363–4368.

[52] R. Van Ham, B. Vanderborght, M. Van Damme, B. Verrelst, and D. Lefeber, "MACCEPA, the mechanically adjustable compliance and controllable equilibrium position actuator: Design and implementation in a biped robot," *Robot. Auton. Syst.*,vol. 55, no. 10, pp. 761–768, 2007.

[53] B. Vanderborght, N. Tsagarakis, R. Van Ham, I. Thorson, and D. G. Caldwell, "MACCEPA 2.0: Compliant actuator used for energy efficient hopping robot Chobino1D," *Auton. Robots*, vol. 31, pp. 55–65, Jul. 2011.

[54] S. Wolf, O. Eiberger, and G. Hirzinger, "The DLR FSJ: Energy based design of a variable stiffness joint," in *Proc. IEEE Int. Conf. Robot. Autom.*, Shanghai, China, May 2011, pp. 5082–5089.
[55] A. H. Memar, N. Mastronarde, and E. T. Esfahani, "Design of a novel variable stiffness gripper using permanent magnets," in *Proc. IEEE Int. Conf. Robot. Automat. (ICRA)*, Singapore, May/Jun. 2017, pp. 2818–2823, doi: 10.1109/ICRA.2017.7989328.
[56] M. I. Awad *et al.*, "Novel passive discrete variable stiffness joint (pDVSJ): Modeling, design, and characterization," in *Proc. IEEE Int. Conf. Robot. Biomimetics (ROBIO)*, Dec. 2016, pp. 1808–1813.
[57] M. Plooij, W. Wolfslag, and M. Wisse, "Clutched elastic actuators," *IEEE/ASME Trans. Mechatronics*, vol. 22, no. 2, pp. 739–750, Apr. 2017.
[58] G. Mathijssen, D. Lefeber, and B. Vanderborght, "Variable recruitment of parallel elastic elements: Series–parallel elastic actuators (SPEA) with dephased mutilated gears," *IEEE/ASME Trans. Mechatronics*, vol. 20, no. 2, pp. 594–602, Apr. 2015.
[59] G. Mathijssen, R. Furnémont, S. Beckers, T. Verstraten, D. Lefeber, and B. Vanderborght, "Cylindrical cam mechanism for unlimited subsequent spring recruitment in series-parallel elastic actuators," in *Proc. IEEE Int. Conf. Robot. Autom. (ICRA)*, May 2015, pp. 857–862.
[60] G. Mathijssen *et al.*, "+SPEA introduction: Drastic actuator energy requirement reduction by symbiosis of parallel motors, springs and locking mechanisms," in *Proc. IEEE Int. Conf. Robot. Autom. (ICRA)*, May 2016, pp. 676–681.
[61] E. J. Rouse, L. M. Mooney, E. C. Martinez-Villalpando, and H. M. Herr, "Clutchable series-elastic actuator: Design of a robotic knee prosthesis for minimum energy consumption," in *Proc. IEEE Int. Conf. Rehabil. Robot.*, Jun. 2013, pp. 1–6.
[62] S. Diller, C. Majidi, and S. H. Collins, "A lightweight, low-power electroadhesive clutch and spring for exoskeleton actuation," in *Proc. IEEE Int. Conf. Robot. Autom.*, May 2016, pp. 682–689.
[63] D. W. A. Rees, *Mechanics of Optimal Structural Design: Minimum Weight Structures*. Hoboken, NJ, USA: Wiley, 2009.
[64] J. Amiguet, S. Sessa, H. Bleuler, and A. Takanishi, "Design of a wearable device for low frequency haptic stimulation," in *Proc. IEEE Int. Conf. Robot. Biomimetics (ROBIO)*, Zhuhai, China, Dec. 2015, pp. 297–302.
[65] M. Bianchi, E. Battaglia, M. Poggiani, S. Ciotti, and A. Bicchi, "A wearable fabric-based display for haptic multi-cue delivery," in *Proc. IEEE Haptics Symp.*, Apr. 2016, pp. 277–283.
[66] M. I. Awad *et al.*, "Passive discrete variable stiffness joint (pDVSJ-II): Modeling, design, characterization and testing towards passive haptic interface,"*ASME J. Mech. Robot.*, vol. 6, p. 68, 2018.
[67] S. Islam, D. Gan, R. Ashour, P. Dario, J. Dias, and L. D. Seneviratne, "Haptics and virtual reality based bilateral telemanipulation of miniature aerial vehicle over open communication network," in *Proc. 18th Int. Conf. Adv. Robot.*, Hong Kong, Jul. 2017, pp. 334–339.
[68] W. Wannasuphoprasit, R. B. Gillespie, J. E. Colgate, and M. A. Peshkin, "Cobot control," in *Proc. IEEE ICRA*, Albuquerque, NM, USA, Apr. 1997, pp. 3571–3576.

MOHAMMAD I. AWAD (S'12–M'18) received the master's degree in mechanical engineering from the Jordan University of Science and Technology, Jordan, in 2011, and the Ph.D. degree in robotics from the Khalifa University of Science and Technology in 2018. He is currently a Post-Doctoral Research Fellow with the Khalifa University Robotics Institute, Khalifa University of Science and Technology.

In 2007, he established his career starting as an automation engineer in a private company in Jordan. During that time, he was also a Research and a Teaching Assistant with the Jordan University of Science and Technology, where he was exposed to work partially in projects related to the industrial consultancy. In 2010, he joined the King Abdullah II Design and Development Bureau and served as a Product Development Engineer. He was involved in developing several military and civilian service vehicles. In 2013, he joined the Masdar Institute for Science and Technology as a Research Associate conducting researches in concentrated solar power control systems and water distillation. Since 2014, he has been a Teaching and Research Associate with the Khalifa University of Science and Technology.

Dr. Awad is a member of the ASME.

DONGMING GAN received the Ph.D. degree based on a joint program from the King's College London and the Beijing University of Posts and Telecommunications in 2009. He is currently an Assistant Professor in mechanical engineering and robotics with the Khalifa University of Science and Technology, Abu Dhabi, United Arab Emirates. His main research interests include fundamental theories of spatial robot mechanisms and their applications in automatic manufacturing, medical robotics and wearable robotics. In particular, he works on novel mechanism design, kinematics solving, dynamics analysis, and reconfiguration of spatial serial and parallel mechanisms. He is an Associate Editor of the Springer journal *Mechanism and Machine Theory*, a Review Editor on the Editorial Board of *Bionics and Biomimetics in Frontiers Journal*, an Editorial Board Member of the *Journal of Applied Mechanical Engineering*, and a member of the American Society of Mechanical Engineers (ASME). He has served on the program committees and symposiums of several international conferences, including the IEEE/ASME Remar 2012, 2015, and 2018, SoSE 2013–2017, Parallel 2014, and ASME MR 2012–2016.

ALI AZ-ZU'BI received the B.Sc. degree in mechatronics engineering from The Hashemite University, Jordan, in 2008, and the Professional master's degree in industrial process automation from Joseph Fourier University, France, in 2011. He was a Research Assistant, where he analyzed and developed a beamforming filter for EEG brain signals until 2012. He later joined the Jordan University of Science and Technology as a Lab Instructor, where he was responsible for developing novel computer-based experimental benches for instrumentation and vibration until 2015. He is currently a Lab Instructor with Khalifa University, United Arab Emirates, where has been teaching mechatronics, control, and design for manufacturability labs. In addition of being actively involved in research on instrumentation, control and robotics as a Certified LabVIEW Developer, his professional and theoretical interests include real-time control and instrumentation, mechatronics, robotics, and CNC manufacturing technologies.

IRFAN HUSSAIN received the second-level master's degree in automation and control technologies from the Politecnico di Torino, Italy, and the M.S. degree in mechatronics engineering from the National University of Sciences and Technology, Pakistan, and the Ph.D. degree with the Department of Information Engineering, University of Siena, Siena, Italy. From 2012 to 2013, he was a Research Assistant with Gyeongsang National University, South Korea. From 2008 to 2011, he was an Assistant Manager of engineering in Trojans, Pakistan. His research interests include mechatronics, bio-robotics, and haptics.

CESARE STEFANINI (M'05) received the M.Sc. degree in mechanical engineering and the Ph.D. degree in microengineering from Scuola Superiore Sant'Anna (SSSA), Pisa, Italy, in 1997 and 2002, respectively. In 2003 he joined as Assistant Professor with the BioRobotics Institute, SSSA in Pontedera, Italy, where he later became an Associate Professor. In 2015, he has been appointed as an Associate Professor with Khalifa University, Abu Dhabi. He has been a Visiting Researcher with the Center for Design Research, University of Stanford. . He is currently the PI of four industrial projects involving large enterprises, a European project on underwater robotics and a national one on bioinspired renewable energy sources. In the recent past, he was the PI of two major European Projects, the first one addressing new bioinspired robotic artifacts, and the second one aimed at developing new high-precision manufacturing technologies for flexible, cost efficient, and eco-friendly mass production of complex shape parts at the micro/meso-scale level. He is also a Founder of a spin-off company active in the field of micro-scale energy and actuation and he is the scientific advisor of a leading company in the field of robotic microsurgery. His research activity is applied to different fields, including small scale biorobotics, actuators for compliant robots, and biomechatronics and micromechatronics for medical and industrial applications. He received international recognitions for the development of novel actuators for microrobots.

He is the author or co-author of over 120 articles on refereed international journals and on international conferences proceedings. He is the inventor of 14 international patents, eight of which industrially exploited by world-leading companies. His Scopus h-index is 21. He is a member of the IEEE Robotics and Automation, Engineering in Medicine and Biology, and Power and Energy Societies.

KINDA KHALAF received the B.S. degree *(summa cum laude)*, the M.S. (Hons.) degree in mechanical engineering and the Ph.D. degree from The Ohio State University, USA. Her Ph.D. thesis was on biomechanics/computational biomechanics, specializing in biomaterials, and dynamic modeling and control. She has held faculty appointments in engineering and medicine at several prestigious universities, including the University of Miami and the American University of Beirut. She currently serves as an Associate Chair of the Department of Biomedical Engineering, Khalifa University, Abu Dhabi. She has numerous publications in the areas of musculoskeletal biomechanics, computational biomechanics, and neuromusculoskeletal modeling and control. She is on the list of International Who Is Who of Professionals. She has received various awards and honors, including the prestigious National Merit Scholar and the Khalifa Award for Education. She is a Founding Member of the IEEE EMBC in United Arab Emirates and a member of many professional organizations.

YAHYA ZWEIRI received the Ph.D. degree from the King's College London in 2003. He is currently the School Director of the Research and Enterprise, Kingston University London, U.K. He is also a Visiting Associate Professor with the Robotics Institute, Khalifa University, United Arab Emirates. He was involved in defense and security research projects in the last 20 years at the Defence Science and Technology Laboratory, King's College London, and the King Abdullah II Design and Development Bureau, Jordan.

His central research focus is interaction dynamics between unmanned systems and unknown environments by means of deep learning, machine intelligence, constrained optimization, and advanced control. He has published over 85 refereed journal and conference papers and filed five patents in USA and U.K. in unmanned systems field.

JORGE DIAS received the Ph.D. degree in electrical engineering with specialization in control and instrumentation from the University of Coimbra, Coimbra, Portugal, in 1994.

He holds his research activities at the Institute of Systems and Robotics, University of Coimbra, and also at the Khalifa University of Science, Technology and Research. His current research areas are computer vision and robotics, with activities and contributions in these fields since 1984. He is currently on the Board of Officers from the Portuguese Chapter for the IEEE Robotics and Automation Society.

LAKMAL D. SENEVIRATNE received B.Sc. (Eng.) and Ph.D. degrees in mechanical engineering from the King's College London (KCL), London, U.K.

He is currently a Professor in mechanical engineering and the Director of the Robotics Institute at Khalifa University. He is also an Emeritus Professor with KCL. His research interests are focused on robotics and autonomous systems. He has published over 300 refereed research papers related to these topics.